We are IntechOpen, the world's leading publisher of Open Access books Built by scientists, for scientists

6,900
Open access books available

185,000
International authors and editors

200M
Downloads

Our authors are among the

154
Countries delivered to

TOP 1%
most cited scientists

12.2%
Contributors from top 500 universities



WEB OF SCIENCE™

Selection of our books indexed in the Book Citation Index in Web of Science™ Core Collection (BKCI)

Interested in publishing with us?
Contact book.department@intechopen.com

Numbers displayed above are based on latest data collected.
For more information visit www.intechopen.com



Chapter

An Experimental Investigation of Al_2O_3-40% TiO_2 Powder Amalgamated via Atmospheric Plasma Spray Coating onto SS316 Substrate and Parameter Optimization Using TLBO Algorithm

Thankam Sreekumar Rajesh

Abstract

SS316 is a commercial stainless steel. MTBF (Mean Time Between Failure) of SS 316 wear prone areas can be effectively increased by ceramic coating. The coating thickness, surface roughness, coating microhardness, abrasion rate, and coating porosity decides the quality and durability in ceramic coating. The current research work explains an experimental investigation to optimize the Atmosphere Plasma Spray process input parameters of Al_2O_3-40%TiO_2 ceramic coatings. Three-level L_{18} Orthogonal Array (OA) design of Experiments (DoE) is used to conduct the current work. The main input parameters considered in the current study are nozzle distance, substrate speed, arc current, carrier gas flow, and coating powder flow rate. The output parameters considered are coating thickness, surface roughness, coating microhardness, abrasion rate, and percentage of porosity. Mathematical models are generated for individual output parameters. AHP (Analytical Hierarchy Process) is effectively used to find out weights for individual output parameters treating them as objective functions, and a combined objective function is generated.

Keywords: atmospheric plasma spray (APS) coating, SS316, teaching learning based optimization (TLBO), Al_2O_3-40%TiO_2

1. Introduction

To achieve increased reliability and performance of damage prone industrial-related components, surface engineering is hugely now applied using large field of new technologies. The quest for higher efficiency and productivity across the entire spectrum of manufacturing and engineering industries has ensured that most of the machine components are subjected to highly harsh environments during routine

IntechOpen

operation [1, 2]. The high deterioration of parts and their ultimate failure has been traced to material damage bought in by hostile environments like high relative motion between mating services, corrosive media, extreme temperatures, and cyclic stresses. As a result of the above, the concept of applying engineered surfaces capable of combating the high degradation phenomena like wear, corrosion, and fatigue to improve component performance, reliability, and life cycle has gained high acceptance in last one decade. To act as a last line of defense, a proactive coating deposited to act as a perfect barrier between the initial surface of the component and the aggressive environment that is exposed during routine operation is now globally acknowledged as an attractive and effective solution to significantly reduce damage.

316 stainless steel is widely used in chemical/petrochemical industry, food processing, pharmaceutical equipment manufacturing, medical devices fabrication, in potable water/wastewater treatment/marine applications and architectures. SS316 composition consists of Chromium 10–14%, Nickel 2–3%, carbon 16–18%, and Molybdenum. In general, the addition of about 2% Molybdenum in SS316 stainless steel provides excellent level of resistance against pitting corrosion and stress corrosion cracking especially in a saline environment compared to SS304. Abrasion and wear resistance is the type of damage which needs to be improved during its application in industrial environment. Abrasion resistance capabilities of SS316 can be highly enhanced by providing a coating of Al_2O_3-40%TiO_2 on an SS316 steel surface by means of atmospheric plasma spraying.

Hence Al_2O_3-40%TiO_2 coating on SS316 surface makes it an ideal combination to combat today's highly drastic and hostile industrial environments where assets are sweating to achieve target of productivity and yield which is always more than 100% of the rated capacity. Even though there is a high level of interest and expectations regarding the fundamentals and development of atmospheric plasma arc spraying, there is a huge gap of reliable as well as dependable models that correlates final engineering properties of coatings such as surface roughness, microhardness, porosity, etc. with variations in critical input process parameters and geometry of deposition process [3].

In the present work, Al_2O_3-40% TiO_2 is coated on SS316 substrates and all the desired critical output parameters are measured and recorded for further analysis.

2. Experimentation details

Justification for the usage of Al_2O_3-40% TiO_2 amalgamated powder.

Al_2O_3-40% TiO_2 amalgamated powder is used for all the experiments conducted during this research work. The use of Al_2O_3-40% TiO_2 justified as it helps to decrease the melting temperature of amalgamated composite powder and hence the final coating exhibits very low porosity % and enhanced fracture toughness compared to 97/3 and 87/13 Al_2O_3 and TiO_2 combinations. The coating generated with Al_2O_3-40% TiO_2 amalgamated powder also possesses high dielectric strength, enhanced wear and heat resistance [4].

2.1 Development of experimental plan

As per the literature review, the following process parameters play a deciding role in the Al_2O_3-TiO_2atmospheric plasma spray process on various substrates.

Major input parameters of a plasma arc spray are below:

1. Carrier gas flow rate (Ar: 20–45 L/min, H_2: 8–14 L/min)
2. Powder feed rate (19–56 g/min)
3. Electric power input/Arc current (250–600 Amps)
4. Substrate rpm
5. Spray distance (70–200 mm)
6. Flame temperature (14000–16,000°C)
7. Composition of working gas
8. Fuel gas to oxygen ratio
9. Powder particle size
10. Powder morphology
11. Pre-spray sand blasting particle size (20/24/60 μm)
12. Bond coat material type (Ni Cr 80/20, 60/40, 70/30)
13. Post spray treatment
14. Substrate temperature (40–200°C)
15. Spray gun Coolant type (Chilled water or normal water, air)
16. Mixing combination of Al_2O_3/TiO_2 (13% Wt TiO_2, 40% Wt TiO_2, 20%Wt TiO_2)
17. Gas injection angle and parameters related with gun
18. Nozzle diameter (6, 6.5, 7, 7.5, 8 mm, GP, GH, GE, G Profiles)
19. Sealing after coating
20. Use of device for coating (Manipulator/robot/manual)
21. RPM of the job, while coating (100–500 RPM)
22. Distance between the substrate and the nozzle (75–125 mm)

The major output parameters are listed below:

1. Porosity %
2. Coating thickness

No	Parameter	Low level	Middle level	High level
1	Spray distance of gun, mm	75	100	125
2	Carrier gas flow, lit./min.	20	30	50
3	Powder flow rate, g/min	25	35	50
4	RPM of the substrate	150	250	350
5	Arc current, A	350	400	500

Table 1.
Input parameters with three levels.

3. Microhardness
4. Abrasion resistance (abrasion rate)
5. Surface roughness
6. Oxidation on surface
7. Microhardness
8. Abrasion resistance, abrasion rate
9. Bonding strength
10. Wear resistance
11. Dielectric strength

After considering the critical requirements of the industry, review of facilities available and thorough literature survey, the following input parameters with three levels are considered for experiments as shown as **Table 1**.

Similarly, the output parameters selected are: coating thickness, surface roughness, microhardness, abrasion rate, and porosity %.

3. Design of experiments

Orthogonal array experimental design proposed by Taguchi can be efficiently used to examine the effect of different input parameters on the critical performance characteristics linked output parameters through compact set of experiments [5]. In-depth understanding of the process, including the minimum, maximum, and current value of the parameter is required to decide the set of input parameters that are highly affecting a process as well as the levels at which these parameters should be varied [6].

After thoroughly understanding the number of input parameters and the number of levels a proper compact can be finalized using the array selector as shown in **Table 2**, by looking at the column and row corresponding to the number of parameters and number of levels.

An L18 orthogonal array is used to carry out all the experiments as shown in **Table 3** considering the five input parameters with three levels. **Table 4** shows the complete experiment plan.

	Number of parameters																	
Number of levels	2	3	4	5	6	7	8	9	10	11	12	13	14	15	16	17	18	19
2	L4	L4	L8	L8	L8	L8	L12	L12	L12	L12	L16	L16	L16	L16	L32	L32	L32	L32
3	L9	L9	L9	L18	L18	L18	L18	L27	L27	L27	L27	L27	L36	L36	L36	L36	L36	L36
4	L16	L16	L16	L16	L32	L32	L32	L32	L32									
5	L25	L25	L25	L25	L25	L50	L50	L50	L50	L50	L50							

Table 2.
Array selector for DoE.

intechopen

Experiment	P1	P2	P3	P4	P5
1	1	1	1	1	1
2	1	2	2	2	2
3	1	3	3	3	3
4	2	1	1	2	2
5	2	2	2	3	3
6	2	3	3	1	1
7	3	1	2	1	3
8	3	2	3	2	1
9	3	3	1	3	2
10	1	1	3	3	2
11	1	2	1	1	3
12	1	3	2	2	1
13	2	1	2	3	1
14	2	2	3	1	2
15	2	3	1	2	3
16	3	1	3	2	3
17	3	2	1	3	1
18	3	3	2	1	2

Table 3.
L18 orthogonal array.

SN	Spray distance mm	Substrate rpm	Arc current A	Carrier gas flow L/min	Powder flow rate g/min
1	75	150	300	20	25
2	75	250	400	30	35
3	75	350	500	40	50
4	125	150	300	30	35
5	125	250	400	40	50
6	125	350	500	20	25
7	175	150	400	20	50
8	175	250	500	30	25
9	175	350	300	40	35
10	75	150	500	40	35
11	75	250	300	20	50
12	75	350	400	30	25
13	125	150	400	40	25
14	125	250	500	20	35
15	125	350	300	30	50
16	175	150	500	30	50
17	175	250	300	40	25
18	175	350	400	20	35

Table 4.
Complete plan of experiments as per L18 OA.

4. Experimental steps

Al_2O_3-40%TiO_2 powder from H C Starck, USA is utilized for coating for all the set of experiments. SS316 substrates are prepared with 27.5 mm diameter and 3 mm thickness plates and pieces of size 75 × 25 ×12 mm are prepared for coating so as to conduct the Abrasion test [7].

Each experiment is carried out with three substrate samples. The substrate samples are assembled in one specially fabricated cartridge [8]. To avoid non-uniformity in thickness, the substrate samples are ground to achieve relatively good finish. Later, sand blasting is carried out on the surface of all substrate samples to ensure proper removal of oxides and other impurities [9, 10]. For sand blasting, fused alumina of grit size 60 μm from Carborandum Universal is used [11, 12]. Al_2O_3-40% TiO_2 powder is deposited on the substrates by using a controlled atmospheric plasma stray system of Metco USA through an SG 100 model Plasma Gun. To ensure the removal of moisture, the amalgamated powder is preheated before the plasma coating process up to 110°C [13].

As pre the L18 orthogonal array DoE, the experiments are conducted. The coating facility arrangement is shown in **Figure 1**. The parameters which are kept constant during the experiment are

Spray nozzle	GP, diameter: 5.43 mm
Grind blasting pressure	2 kg/cm^2
Substrate exposure to gun	30 s
Primary gas pressure	100 Psi
Secondary gas pressure	80 Psi

The substrate samples are cleaned after the coating with ethanol and properly dried to eliminate accumulation of moisture [14]. As per ASTM B499-92014 [15], coating thickness is measured. An ultrasonic thickness gauge is used for this purpose. Using Mitutoyo surface roughness tester SV-C3100, surface roughness is measured as per ASTM D127 2013 [16]. The surface testing probe is applied on the coating surface for a length of 15 mm with a pitch of 0.001 mm. The scanning speed is kept constant at 2.0 mm/s. Microhardness is measured as per ASTM B 578-872,015 [17] by Metatech MVH-1. To measure porosity as well as microhardness, the samples are sectioned by wire cutting as well as slow speed grinding.

Later, molds are prepared using Bain mount-3 molding machine supplied by Chennai Matco. The substrate surfaces on the mold are polished with emery papers

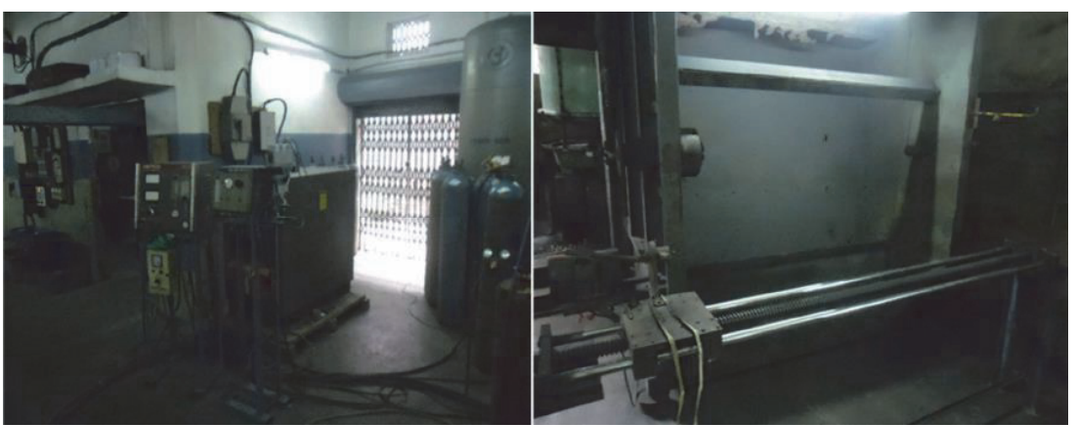


Figure 1.
Coating facility arrangement.

ranging from 150 grit up to 2000 grit so as to get scale free and super finished surface. The porosity is measured using an Image Analysis Software as shown in **Figure 2**. The JPG images of the coatings are taken by using an electronic microscope OLIMBUS GX51 as per ASTM E2109-012014 [18]. A sample image of the sectioned coating surface is shown as **Figure 3**. Abrasion rate is measured on Abrasion test rig TR-50 as per ASTM G65 2000 [19] with 1000 g. as pre-load. **Figure 4** shows one of the abrasion test in progress. This test method covers laboratory procedures for determining the resistance of coating materials to scratching abrasion by means of the dry sand/rubber wheel test. Abrasion test results are reported as weight loss in grams for 20 revolutions of the wheel for a particular substrate. Materials of higher abrasion rate and high weight loss show a lower abrasion resistance.

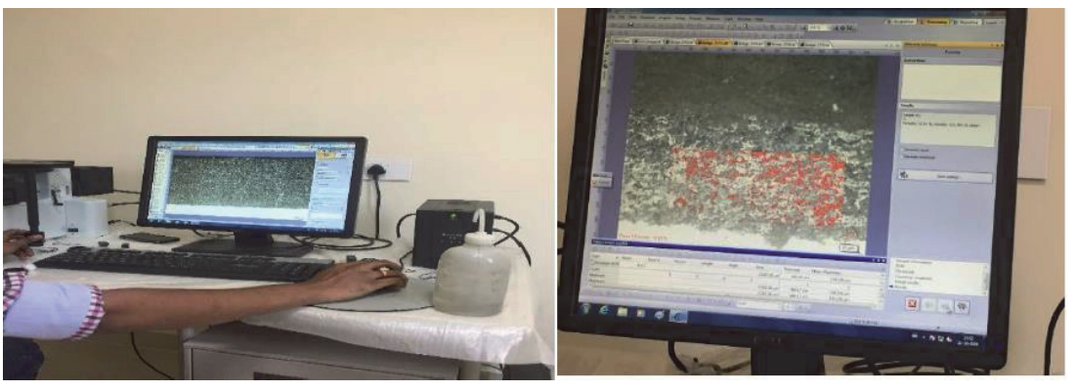


Figure 2.
Measurement of porosity in progress.

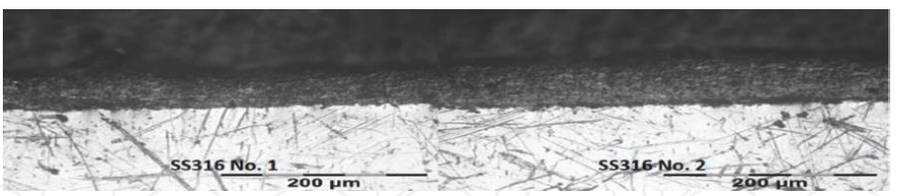


Figure 3.
Sample photograph of the sectioned coated surface.



Figure 4.
Abrasion test in progress.

4.1 Details of coating output parameters

The measured values of coating thickness, surface roughness, microhardness, abrasion rate, and porosity % are given in **Table 5**.

To generate mathematical models for each of the output parameters, excel data analysis is used [18]. The mathematical models generated for all the output parameters are shown below as Eqs. (1) and (2).

$$\begin{aligned}\text{T, Thickness } (\mu\text{m}) = {} & 1934.148 - 27.5317 \times \text{D} - 4.39986 \times \text{N} - 2.41271 \times \text{A} \\ & + 23.17571 \times \text{G} + 12.19609 \times \text{P} + 0.017778 \times \text{D} \times \text{N} \\ & + 0.009069 \times \text{D} \times \text{A} + 0.265778 \times \text{D} \times \text{G} + 0.287119 \times \text{D} \times \text{P} \\ & + 0.00872 \times \text{N} \times \text{A} - 0.02146 \times \text{N} \times \text{G} + 0.015764 \times \text{N} \times \text{P} \\ & + 0.019442 \times \text{A} \times \text{G} - 0.00704 \times \text{A} \times \text{P} - 1.40365 \times \text{G} \times \text{P}\end{aligned} \tag{1}$$

$$\begin{aligned}\text{R, Roughness } (\mu\text{m}) = {} & 13.669392 + 0.029373 \times \text{D} - 0.007159 \times \text{N} - 0.005758 \times \text{A} \\ & - 0.52605 \times \text{G} - 0.093101 \times \text{P} - 0.000006 \times \text{D} \times \text{N} \\ & - 0.000184 \times \text{D} \times \text{A} + 0.001429 \times \text{D} \times \text{G} + 0.00035 \times \text{D} \\ & \times \text{P} + 0.000029 \times \text{N} \times \text{A} - 0.000099 \times \text{N} \times \text{G} + 0.000056 \\ & \times \text{N} \times \text{P} + 0.000789 \times \text{A} \times \text{G} - 0.000001 \times \text{A} \times \text{P} \\ & + 0.000907 \times \text{G} \times \text{P}\end{aligned} \tag{2}$$

No	Mean coating thickness, μm	Mean surface roughness, μm	Mean microhardness HV	Mean abrasion rate, g	Mean porosity, %
1	343.33	5.2	953	0.1602	14.2243
2	186.67	4.22	929	0.1322	11.5634
3	226.67	5.46	906	0.1998	13.2112
4	170	4.48	749	0.1023	18.0264
5	433.33	4.54	802	0.0601	11.4133
6	236.67	5.1	953	0.0855	9.5114
7	286.67	4.33	766	0.0973	14.7045
8	206.67	4.36	716	0.1022	18.9231
9	376.67	5.36	821	0.135	15.0654
10	366.67	4.72	766	0.0355	9.0012
11	516.67	4.35	841	0.0546	36.2234
12	600	4.74	841	0.0788	17.2133
13	416.67	4.36	821	0.0786	19.4231
14	476.67	4.39	802	0.0688	19.7324
15	323.33	4.42	821	0.1001	25.3381
16	346.67	3.95	802	0.1001	22.1099
17	203.33	5.43	766	0.1255	10.5224
18	283.33	5.03	784	0.0979	21.3422

Table 5.
The values of measured output parameters–SS316.

$$\text{H, Microhardness (HV)} = 2866.016 - 14.81975 \times D - 5.535376 \times N - 2.302965 \times A - 6.870915 \times G - 11.56905 \times P + 0.010359 \times D \times N - 0.002454 \times D \times A + 0.207755 \times D \times G + 0.180859 \times D \times P + 0.010923 \times N \times A - 0.016017 \times N \times G + 0.030724 \times N \times P + 0.016899 \times A \times G + 0.00575 \times A \times P - 0.54882 \times G \times P \quad (3)$$

$$\text{A, Abrasion rate (g)} = 0.84561453 + 0.00023070 \times D - 0.00160816 \times N - 0.00127953 \times A - 0.00654575 \times G - 0.01238197 \times P - 0.00000033 \times D \times N + 0.00000114 \times D \times A - 0.00001169 \times D \times G - 0.00000214 \times D \times P + 0.00000106 \times N \times A + 0.00002805 \times N \times G + 0.00001562 \times N \times P + 0.00000362 \times A \times G + 0.00002127 \times A \times P - 0.00001584 \times G \times P \quad (4)$$

$$\text{P, Porosity (\%)} = 43.36101115 - 0.55405377 \times D + 0.03082400 \times N - 0.18845218 \times A + 1.40724984 \times G + 0.74786458 \times P + 0.00002005 \times D \times N + 0.00120547 \times D \times A + 0.00284447 \times D \times G - 0.00062184 \times D \times P - 0.00004973 \times N \times A - 0.00199498 \times N \times G + 0.00226109 \times N \times P + 0.00060184 \times A \times G + 0.00091991 \times A \times P - 0.04473134 \times G \times P \quad (5)$$

where, D = spray distance; N = substrate rpm; A = arc current; G = carrier gas flow rate; P = powder flow rate.

The values of roughness, abrasion rate and porosity are considered non-beneficial and the values of thickness and hardness are considered as beneficial.

4.2 Confirmation experiments

For conducting confirmation tests, three trial samples of SS316 are used. The random values for all the input parameters, in between the maximum and

Spray distance mm	Substrate rpm	Arc current A	Carrier gas flow L/min	Powder flow rate g/min	Coating thickness µm	Predicted values µm	% variation
150	300	450	35	30	278.33	306.8094	10.2322
160	225	325	25	30	206.33	218.2186	5.7619
80	190	425	35	40	322.67	296.4082	8.1388

Table 6.
Measured and predicted values – Thickness, SS316.

Spray distance mm	Substrate rpm	Arc current A	Carrier gas flow L/min	Powder flow rate g/min	Coating roughness µm	Predicted values µm	% Variation
100	200	350	25	40	4.23	4.476552	5.8286
150	300	450	35	30	4.38	5.264112	20.1852
160	225	325	25	30	5.02	5.577542	11.1064

Table 7.
Measured and predicted values – Roughness, SS316.

Spray distance mm	Substrate rpm	Arc current A	Carrier gas flow rate L/min	Powder flow rate g/min	Hardness HV	Predicted values HV	% Variation
150	300	450	35	30	894	914.1079	2.2492
160	225	325	25	30	578	624.3352	8.0165
80	190	425	35	40	642	770.9902	20.0919

Table 8.
Measured and predicted values – Microhardness, SS316.

Spray distance mm	Substrate rpm	Arc current A	Carrier gas flow L/min	Powder flow rate g/min	Abrasion rate g	Predicted values g	% Variation
115	180	325	25	30	0.0911	0.088834	2.4868
120	215	425	35	40	0.0987	0.118253	19.8107
85	295	495	25	45	0.1265	0.125752	0.5911

Table 9.
Measured and predicted values – Abrasion rate, SS316.

Spray distance mm	Substrate rpm	Arc current A	Carrier gas flow rate L/min	Powder flow rate g/min	Porosity %	Predicted values %	% Variation
80	170	315	25	30	21.33	18.52049	13.1802
95	190	425	35	40	20.01	18.41184	7.9868
140	200	480	35	45	9.56	10.53198	10.1532

Table 10.
Measured and predicted values – Porosity %, SS316.

minimum levels are taken to conduct the confirmation tests. The predicted values using the proposed model along with the measured output parameters values for three samples are given in **Tables 6–10**. The percentage variation between the actual and predicted values are also shown in the tables.

5. SN analysis

To determine the effect each variable has on the output, the signal-to-noise ratio, or the SN number, needs to be calculated for each experiment conducted. In the equations below, y_i is the mean value and s_i is the variance. y_i is the value of the performance characteristic for a given experiment. More details about SN analysis is given in https://google site sn analysis design of experiments.

SN ratio values for coating thickness on SS316 substrate are calculated for each parameter and level. The values are tabulated as shown in **Table 11**.

Spray distance has a significant effect on the coating thickness. Carrier gas flow is the next dominant parameter in the case of coating thickness. Similarly, SN ratio values are calculated for surface roughness for each parameter and level for all the output parameters as shown in **Table 12**. In the case of surface roughness, carrier

gas flow has a significant effect. Substrate rpm is the next influencing parameter as per R value. The spray distance has a significant effect on the microhardness as shown in **Table 13**. The next dominant parameter in the case of microhardness is rpm. For coating abrasion rate, spray distance is the most dominating parameter and then comes the rpm as shown in **Table 14**. In the case of coating porosity % as

	Spray distance	Substrate rpm	Arc current	Carrier gas flow rate	Powder flow rate
Level 1	50.73	49.83	49.58	50.7	49.77
Level 2	50.16	49.74	50.72	48.81	49.24
Lvel 3	48.83	50.15	49.42	50.2	50.71
Δ R	1.90	0.41	1.29	1.89	1.47
Rank	1	5	4	2	3

Table 11.
SN ratio matrix and ΔR values of coating thickness, SS316.

	Spray distance	Substrate rpm	Arc current	Carrier gas flow rate	Powder flow rate
Level 1	13.56	13.05	13.72	13.47	13.71
Level 2	13.14	13.12	13.12	12.78	13.41
Level 3	13.46	13.99	13.32	13.9	13.03
Δ R	0.42	0.94	0.6	1.12	0.68
Rank	5	2	4	1	3

Table 12.
SN ratio matrix and ΔR values of coating roughness, SS316.

	Spray distance	Substrate rpm	Arc current	Carrier gas flow rate	Powder flow rate
Level 1	58.79	58.14	58.3	58.55	58.45
Level 2	58.3	58.13	58.3	58.14	58.13
Level 3	57.79	58.61	58.28	58.19	58.3
Δ R	1.01	0.48	0.03	0.42	0.32
Rank	1	2	5	3	4

Table 13.
SN ratio matrix and ΔR values of microhardness, SS316.

	Spray distance	Substrate rpm	Arc Current	Carrier gas flow l/min	Powder flow rate g/min
Level 1	−20.63	−21.17	−19.4	−21.03	−19.88
Level 2	−21.82	21.39	−21.1	−19.87	−21.2
Level 3	−19.27	−19.16	−21.23	−20.82	−20.65
Δ R	2.55	2.23	1.84	1.16	1.32
Rank	1	2	3	5	4

Table 14.
SN ratio matrix and ΔR values of coating abrasion rate, SS316.

	Spray distance	Substrate rpm	Arc current	Carrier gas flow rate	Powder flow rate
Level 1	23.62	23.88	25.24	24.94	23.18
Level 2	24.26	24.25	23.8	25.27	23.59
Level 3	24.39	24.15	23.23	22.07	25.51
Δ R	0.77	0.37	2.01	3.2	2.33
Rank	4	5	3	1	2

Table 15.
SN ratio matrix and ΔR values of porosity %, SS316.

shown in **Table 15**, the most dominating parameter is carrier gas flow. The next parameter which effects the most is powder flow rate.

6. Application of teaching learning based optimization (TLBO)

An advanced optimization method, known as Teaching-Learning-Based Optimization (TLBO) is applied, to determine the best values of input parameters to obtain global optimum output parameters. TLBO is applied individually to each of the developed mathematical models given by Eqs. (1)–(5). Rao et al., proposed TLBO, which is based on the effect of influence of a teacher on the output of learners in a class. Teaching-learning ability of teacher and learners in a class room is mimicked in this algorithm [20, 21]. There are two modes of learning in this algorithm, interacting with other learners (known as learner phase) and through teacher (known as teacher phase).One of the attractive features of this algorithm is its algorithm-specific parameter-less concept. The algorithm is widely preferred among researchers due to its simplicity and its ability to provide the global optimum solutions in comparatively less number of function evaluations. Further details about the TLBO algorithm can be found at https://sites.google.com/site/tlborao.

To execute TLBO algorithm for the optimisation of individual objective functions, a population size of 10 and 100 number of iterations with 30 independent runs is considered. The global optimum values for individual objective functions of T (Coating thickness), R (Surface roughness), H (Microhardness), Ab (Abrasion rate) and Po (Porosity %) obtained after applying TLBO are given in **Table 16**.

Values obtained by applying the TLBO algorithm for the individual objective functions of T (Thickness), R (Roughness), H (Microhardness), Ab (Abrasion rate

Objective function (Output parameter)	Optimum values of input parameters					Value of the objective function
	Spray distance	Substrate rpm	Arc current	Carrier gas flow	Powder flow rate	
Coating thickness	175	350	500	40	50	1068.8 μm
Surface roughness	75	350	300	40	50	1.1503 μm
Microhardness	175	350	500	40	50	1396 HV
Abrasion rate	75.34	150	300	40	50	0.0073 g
Porosity %	75	150	500	20	25	1.4935%

Table 16.
Optimized output parameter values obtained by applying TLBO.

and Po (Porosity %) are 1068.8 μm, 1.1503 μm, 1396 HV, 0.0073 g, and 1.4935% respectively. For each of the output parameters, the corresponding values of process input parameters are also given in **Table 16**. It can be observed from **Table 16** that the optimum values of input parameters for getting optimum value of a particular objective (i.e., output parameter) are not the same for the other objectives. In real industrial situations, it is required to find the set of optimum values of input parameters that satisfies all the objectives simultaneously. Hence, the problem becomes a multi-objective problem with the ranges of the input parameters as constraints. In the current work, a combined objective function is formed considering all the five objectives simultaneously. This is called a priori approach of solving the multi-objective optimization problems.

7. Formation of combined objective function

A pirori approach is used by forming a combined objective function, involving all the three objectives and this function is solved by applying TLBO algorithm for the given ranges of the input parameters.

$$Z_{max} = \omega_T * \frac{T}{T_{max}} + \omega_H * \frac{H}{H_{max}} - \omega_{Ab} * \frac{Ab}{Ab_{min}} - \omega_{Po} * \frac{Po}{Po_{min}} - \omega_R * \frac{R}{R_{min}} \quad (6)$$

The normalized weights of each output parameters are calculated using AHP (Arithmetic Hierarchy Method) [22] and these are ω_T = 0.4027, ω_R = 0.0694 ω_H = 0.2595 ω_{Ab} = 0.1342 and ω_{Po} = 0.1342. The weights are applied to combined objective function as given below in Eq. (7). For more details about AHP method pl. refer https://google site AHP Saaty.

$$\begin{aligned} Z_{max} = {} & [(0.4027/1068.8) \times (1934.148 - 27.5317 \times D - 4.39986 \times N \\ & -2.41271 \times A + 23.17571 \times G + 12.19609 \times P + 0.017778 \times D \times N \\ & + 0.009069 \times D \times A + 0.265778 \times D \times G + 0.287119 \times D \times P \\ & + 0.00872 \times N \times A - 0.02146 \times N \times G + 0.015764 \times N \times P \\ & + 0.019442 \times A \times G - 0.00704 \times A \times P - 1.40365 \times G \times P)] \\ & + [(0.2595/1396) \times (2866.016 - 14.81975 \times D - 5.535376 \times N \\ & -2.302965 \times A - 6.870915 \times G - 11.56905 \times P + 0.010359 \times D \\ & \times N - 0.002454 \times D \times A + 0.207755 \times D \times G + 0.180859 \times D \\ & \times P + 0.010923 \times N \times A - 0.016017 \times N \times G + 0.030724 \times N \\ & \times P + 0.016899 \times A \times G + 0.00575 \times A \times P - 0.54882 \times G \times P)] \\ & - (0.1342/0.0073) \\ & \times (0.84561453 + 0.00023070 \times D - 0.00160816 \times N \\ & -0.00127953 \times A - 0.00654575 \times G - 0.01238197 \times P \\ & - 0.00000033 \times D \times N + 0.00000114 \times D \times A - 0.00001169 \\ & \times D \times G - 0.00000214 \times D \times P + 0.00000106 \times N \times A \\ & + 0.00002805 \times N \times G + 0.00001562 \times N \times P + 0.00000362 \\ & \times A \times G + 0.00002127 \times A \times P - 0.00001584 \times G \times P)] \\ & - [(0.1342/1.4935) \times (43.36101115 - 0.55405377 \times D \\ & +0.03082400 \times N - 0.18845218 \times A + 1.40724984 \times G \\ & + 0.74786458 \times P + 0.00002005 \times D \times N + 0.00120547 \times D \\ & \times A + 0.00284447 \times D \times G - 0.00062184 \times D \times P \\ & - 0.00004973 \times N \times A - 0.00199498 \times N \times G + 0.00226109 \\ & \times N \times P + 0.00060184 \times A \times G + 0.00091991 \times A \times P \\ & - 0.04473134 \times G \times P)] \\ & - [(0.0694/1.1503) \times (13.669392 + 0.029373 \times D - 0.007159 \times N \end{aligned}$$

$$-0.005758 \times A - 0.52605 \times G - 0.093101 \times P - 0.000006 \times D \times N - 0.000184 \times D \times A + 0.001429 \times D \times G + 0.00035 \times D \times P + 0.000029 \times N \times A - 0.000099 \times N \times G + 0.000056 \times N \times P + 0.000789 \times A \times G - 0.000001 \times A \times P + 0.000907 \times G \times P)] \quad (7)$$

TLBO algorithm can be again applied on the combined objective function and after n number of iterations with independent runs to achieve the global optimum value of coefficient Z_{max} and the corresponding values of the optimum input parameters can be arrived.

8. Conclusion

In the field of atmospheric plasma coating with Al_2O_3-40%TiO_2, mathematical modeling and its optimization is very rare. Mathematical models are generated in the present work using regression analysis for all the output parameters in terms of input parameters. The mathematical models developed will work as effective tools for manufactures to predict the effect of input parameters on output parameters within the considered ranges. Based on this model, they can take decisions and hence costly trials can be avoided to a very large extent. Confirmation tests are also carried out in the present work for each of the output parameters. The confirmation tests have given near about the same values compared to the predicted values and the percentage of error is negligible.

The optimization is effectively carried out using teaching-learning-based optimization (TLBO) algorithm for each output parameter individually. A combined objective function is generated and this combined objective function can be again optimized using TLBO algorithm to get global optimum values of input parameters considering all the output parameters simultaneously. The TLBO algorithm has proved its effectiveness and simplicity in solving the multi-objective optimization problems. The AHP method is applied to decide the weights for the individual objective functions in the combined objective function in a systematic way and it takes into account the preferences of the decision maker. It is also concluded that a change in the weights of the individual objective functions in the combined objective function may give different sets of optimum values of input parameters.

Author details

Thankam Sreekumar Rajesh
SVNIT, Surat, Gujarat, India

*Address all correspondence to: rajeshtsreekumar@gmail.com

IntechOpen

© 2020 The Author(s). Licensee IntechOpen. This chapter is distributed under the terms of the Creative Commons Attribution License (http://creativecommons.org/licenses/by/3.0), which permits unrestricted use, distribution, and reproduction in any medium, provided the original work is properly cited. CC BY

References

[1] Ctibor P, Stengl V, Pis I, Zahoranova T, Nehasil V. Plasma sprayed TiO2: The influence of an electric supply on relations among stoichiometry, surface state and photo catalytic decomposition of acetone. Ceramics International. 2012;**38**: 3453-3458

[2] Datta S, Pratihar DK, Bandyopadhyay PP. Modelling of plasma spray coating process using statistical regression analysis. International Journal of Advanced Manufacturing Technology. 2013;**65**: 967-980

[3] Forghani SM, Ghazali MJ, Muchtar A, Daud AR. Mechanical properties of plasma sprayed nanostructured TiO2 coatings on mild steel. Ceramics International. 2014;**40**: 7049-7056

[4] Ghazali MJ, Forghani SM, Hassanuddin N, Muchtar A, Daud AR. Comparative wear study of plasma sprayed TiO2 and Al2O3–TiO2 on mild steels. Integrated Tribology International. 2016;**93**:681-686

[5] Hazra S, Bandyopadhyay PP. Scratch induced failure of plasma sprayed alumina based coatings. Materials and Design. 2012;**35**:243-250

[6] Morks MF, Akimoto K. The role of nozzle diameter on the microstructure and abrasion wear resistance of plasma sprayed Al2O3/TiO2 composite coatings. Journal of Manufacturing Processes. 2008;**10**:1-5

[7] Mishra NK, Mishra SB, Kumar R. Oxidation resistance of low-velocity oxy fuel-sprayed Al2O3-13TiO2 coating on nickel-based superalloys at 800 °C. Surface and Coating Technology. 2014; **260**:23-27

[8] Paneerselvam R. Design and Analysis of Experiments. New Delhi: PHI Learning Pvt. Ltd.; 2012

[9] Ramachandran CS, Balasubramanian V, Ananthapadmanabhan PV, Viswabaskaran V. Influence of intermixed interfacial layers on the thermal cycling behavior of atmospheric plasma sprayed lanthanum zirconate based coatings. Ceramics International. 2012;**38**:4081-4096

[10] Rico A, Poza P, Rodriguez J. High temperature tribological behaviour of nanostructured and conventional plasma sprayed alumina-titania coatings. Vacuum. 2012;**888**:1-6

[11] Saravanan P, Selvarajan V, Joshi SV, Sundararajan G. Experimental design and performance analysis of alumina coatings deposited by a detonation spray process. Journal of Applied Physics. 2001;**34**:131-140

[12] Sathish S, Geetha M, Aruna ST, Balaji N, Rajam KS, Asokamani R. Sliding wear behaviour of plasma sprayed nanoceramic coatings for biomedical applications. Wear. 2011; **271**:934-941

[13] Sathish S, Geetha M, Aruna ST, Balaji N, Rajam KS, Asokamani R. Studies on plasma sprayed bilayered ceramic coatings for bio-medical Ti-13Nb-13Zr ally. Ceramics International. 2011;**37**:1333-1339

[14] Christel P, Lech P, Murel B, Peirre C. Design of experiments in thermal spraying. A review. Surface and coatings Technology. 2008;**202**: 4483-4490

[15] ASTM B499-09. Standard Test Method for Measurement of Coating

Thicknesses by the Magnetic Method. 2014. Available from: www.astm.org

[16] ASTM D7127. Standard Test Method for Measurement of Surface Roughness of Abrasive Blast Cleaned Metal Surfaces Using a Portable Stylus Instrument. 2013. Available from: www.astm.org

[17] ASTM B578-87. Standard Test Method for Microhardness of Electroplated Coatings. 2015. Available from: www.astm.org

[18] ASTM E2109-0. Standard Test Methods for Determining Area Percentage Porosity in Thermal Sprayed Coatings. 2014. Available from: www.astm.org

[19] ASTM G65. Standard Test Method for Measuring Abrasion Using the Dry Sand/Rubber Wheel Apparatus. 2000. Available from: www.astm.org

[20] Rao RV. Teaching Learning Based Optimization Algorithm and its Engineering Applications. Switzerland: Springer International Publishing; 2016

[21] Rao RV. Review of applications of TLBO algorithm and a tutorial for beginners to solve the unconstrained and constrained optimization problem, Decision Science Letters; 2015

[22] Saaty TL. Fundamentals of the Analytic Hierarchy Process. Pittsburg: RWS Publications; 2000